Eur Spine J (2002) 11 (Suppl. 2) : S115–S123
DOI 10.1007/s00586-002-0481-z

ORIGINAL ARTICLE

Total disc replacement arthroplasty using the AcroFlex lumbar disc: a non-human primate model

Bryan W. Cunningham
Gary L. Lowery
Hassan A. Serhan
Anton E. Dmitriev
Carlos M. Orbegoso
Paul C. McAfee
Robert D. Fraser
Raymond E. Ross
Samir S. Kulkarni

Received: 26 June 2002
Accepted: 3 July 2002
Published online: 20 August 2002
© Springer-Verlag 2002

B.W. Cunningham (✉) · A.E. Dmitriev
P.C. McAfee
Orthopedic Biomechanics Laboratory,
Department of Orthopaedic Surgery,
Union Memorial Hospital,
201 East University Pkwy,
Baltimore, MD 21218, USA
e-mail: bcspine@aol.com,
Tel.: +1-410-5542914,
Fax: +1-410-5542408

G.L. Lowery · S.S. Kulkarni
Research Institute International,
Phoenix, Arizona, USA

H.A. Serhan
DePuy-Acromed Inc.,
Raynham, Massachusetts, USA

C.M. Orbegoso
Department of Pathology,
Union Memorial Hospital,
Baltimore, Maryland, USA

R.D. Fraser
The University of Adelaide,
South Australia, Australia

R.E. Ross
Hope Hospital, Manchester, UK

Abstract Using a non-human primate model, the current study was undertaken to investigate the efficacy of the AcroFlex lumbar disc as an intervertebral disc prosthesis, based on biomechanical, histopathologic and histomorphometric analyses. A total of 20 mature male baboons (Papio cynocephalus, mean weight 30 kg) were randomized into two equal groups based on post-operative time periods of 6 (n=10) and 12 months (n=10). Each animal underwent an anterior transperitoneal surgical approach to the lumbar spine, with intervertebral reconstructions performed at L3-L4 and L5-L6 using the following techniques: (1) tricortical iliac autograft and (2) AcroFlex lumbar disc. The two treatments were equally randomized between the non-contiguous operative lumbar levels. Post-mortem analysis included histopathologic assessment of the systemic reticuloendothelial tissues, multi-directional flexibility testing of the operative functional spinal units and quantitative histological analysis of trabecular bone coverage at the prosthesis endplates. Data were statistically compared using a one-way ANOVA with the Student-Newman-Keuls test. All animals survived the operative procedure and post-operative interval without significant intra- or peri-operative complications. Histopathologic analysis of the paraffin-embedded systemic reticuloendothelial tissues indicated no significant pathologic changes at the 6- or 12-month intervals. Plain film radiographic analysis showed no lucencies or loosening of any prosthetic vertebral endplate. Biomechanical testing of the 6-month autograft, reconstructions with AcroFlex lumbar disc and non-operative control (n=10) intact motion segments indicated no significant differences in peak range of motion (ROM) in axial compression. However, axial rotation produced significantly lower ROM for the autograft treatment compared to the intact and AcroFlex groups (P<0.05). The most significant differences in peak ROM were noted between all treatment groups under flexion/extension and lateral bending loading modalities (P<0.05). By 12 months, the intact condition indicated significantly more motion in all bending modes compared to the AcroFlex and autograft treatments, which were not statistically different from each other (P>0.05). Gross histopathologic analysis of the AcroFlex disc prosthesis demonstrated excellent ingrowth at the level of the implant-bone interface, without evidence of fibrous tissue or synovium. BioQuant histomorphometric analysis at the metal-bone interface (bone contact area/total endplate area) indicated the mean ingrowth was 54.59± 13.24% at 6 months and 56.79± 5.85% at 12 months. Radiographic analysis showed no lucencies or loosening of the AcroFlex vertebral

endplate. Based on multi-directional flexibility testing, motion was preserved in axial rotation, but significantly diminished in the other bending modalities, particularly at the 12-month interval. This effect may be secondary to the limited surface area of device-vertebral endplate contact. Histomorphometric analysis of porous ingrowth coverage at the vertebral bone-metal interface was more favorable for total disc arthroplasty compared to historical reports of cementless femoral components. This project serves as the first comprehensive in vivo investigation into the AcroFlex disc prosthesis, and establishes an excellent research model in the evaluation of total disc replacement arthroplasty.

Keywords Total disc replacement arthroplasty · Animal model · Biomechanics · Histomorphometry · Porous ingrowth

Introduction

Total disc replacement arthroplasty is the next frontier in the surgical management of intervertebral disc pathology. As an alternative to interbody arthrodesis, an artificial disc serves to replace the symptomatic degenerated disc, restore the functional biomechanical properties of the motion segment, and protect neurovascular structures. To this end, the implanted device should encourage osseointegration at the bone-metal interface, re-establish normal kinematics to the functional spinal unit and promote an anterior/posterior column load-sharing environment.

To date, disc replacement technology has focused on two fundamental design strategies with regard to spinal kinematics: (1) unconstrained (mobile bearing core) prosthesis, and (2) constrained (fixed axis of rotation) prosthesis. Unconstrained devices (e.g. SB Charité III) are consistent with the principles of a mobile bearing arthroplasty [3], as the ultra-high molecular weight polyethylene core is able to translate between the vertebral endplates [34]. This design strategy allows for six-degrees-of-freedom segmental motion, with translations and rotations about three independent axes, and markedly diminishes the stress concentration at specific points on the polyethylene core, reducing the incidence of "cold flow" [4]. Constrained devices, in contra-distinction, typically permit rotation in all planes; however, they include a fixed axis of rotation, which limits segmental translation under flexion-extension and lateral bending conditions (e.g. ProDisc). This constrained design concept is thought to minimize anteroposterior shear forces at the operative facet level, while permitting unconstrained rotational motion of the operative segment.

The AcroFlex lumbar disc (Depuy-AcroMed, Inc, Raynham, Mass.) – an unconstrained design – is composed of porous coated titanium endplates and a polyolefin rubber core. Using an in vivo non-human primate model, the current study was undertaken to investigate the nature and magnitude of porous osseointegration following total disc replacement arthroplasty using the AcroFlex lumbar disc, with success criteria based on biomechanical, histopathologic and histomorphometric analyses.

Materials and methods

Animal research permission

The Institutional Animal Care and Use Committee (IACUC) at the Southwest Foundation for Biomedical Research (SFBR), San Antonio, Texas granted approval for this 20-animal project.

Animal model and surgical preparation

A total of twenty skeletally mature male baboons (Papio cynocephalus, 8–10 years old, mean weight 35 kg) were included in this study and followed for a period of 6 (n=10) and 12 (n=10) months post-operatively. Following normal health status determination, each animal was sedated with intravenous (IV) injection of ketamine (10 mg/kg) and diazepam (0.15 mg/kg) anesthetic medications, followed by endotracheal intubation and general anesthesia using 1.5–2.0% isoflurane. With the animal positioned supine, the anterior abdominal lumbar region was shaved, aseptically prepared and draped in sterile fashion. Prophylactic antibiotics (cefazolin sodium 1 g, IV) and analgesics (Butorphenol 125 mg/kg, IV) were administered pre- and post-operatively.

Surgical technique and treatment groups

Tricortical iliac crest bone graft was obtained from each animal using standard technique. Surgical exposure consisted of a 10- to

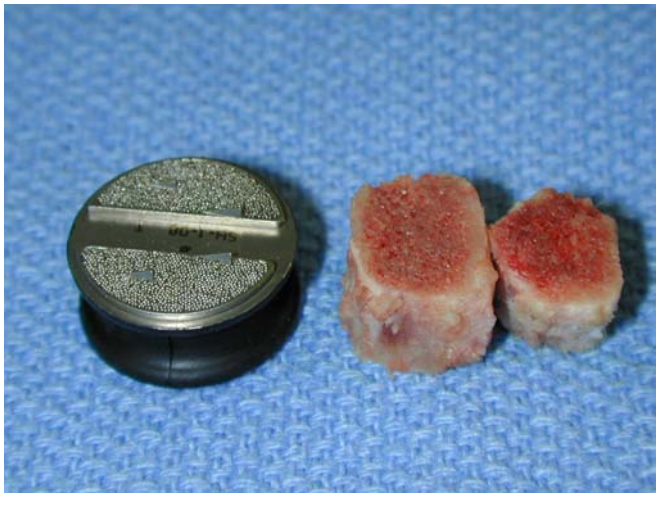

Fig. 1 View of the AcroFlex lumbar disc prosthesis (11 mm height × 20 mm diameter) and tricortical autogenous graft used for intervertebral reconstructions

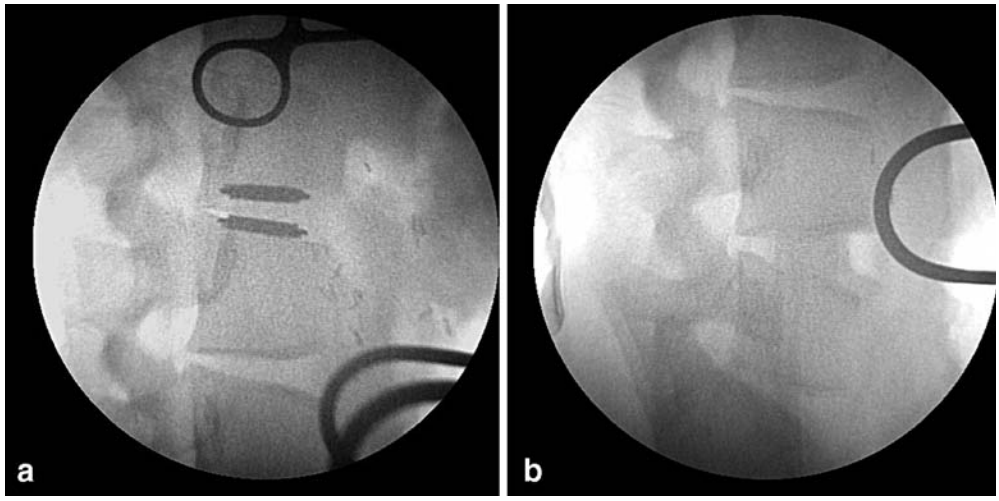

Fig. 2 Lateral fluoroscopic view confirming proper placement of an autograft treatment at L5-L6 (**b**) and AcroFlex disc at L3-L4 (**a**)

15-cm incision along the abdominal midline, followed by soft tissue dissection to permit transperitoneal exposure of the anterior lumbar spine. Blunt dissection using ligatures, Cobb elevator and electrocautery were performed as needed to expose the anterior aspects of the L3-L4 and L5-L6 intervertebral disc spaces. The anterior longitudinal ligament and anterior annulus were incised, followed by complete discectomy including the inner annulus and nucleus pulposus. A special box chisel was used to partially decorticate the vertebral endplates and ensure optimal contact at the bone-implant interface. The two randomized implant treatments were: (1) AcroFlex lumbar disc and (2) tricortical iliac crest (Fig. 1).

A custom distractor was utilized to insert the specially manufactured AcroFlex disc according to the manufacturer's guidelines, while implantation of the iliac crest graft was performed at the other non-contiguous level, using similar technique. The treatments were equally randomized between the two non-contiguous levels, with final positions verified with anteroposterior and lateral fluoroscopic images (Fig. 2).

Following the surgical procedure, the fascia and underlying muscle were closed in an interrupted fashion using 1.0 Vicryl, and the skin approximated using 2.0 Vicryl. Blood loss, operative times and intra- and peri-operative complications were quantified. Ambulatory activities and wound healing were monitored daily and all animals received analgesics and prophylactic antibiotics for the first 10 days post-operatively. Animals were humanely euthanized at the appropriate post-operative time interval, using an overdose (150 mg/kg, IV) of concentrated pentobarbital sodium (concentration=390 mg/ml). Systemic tissues – inguinal, periaortic and mesenteric lymph nodes, lungs, heart, liver, kidneys, spleen and pancreas – and spinal column were then carefully dissected for subsequent histopathologic examination.

Material specifications

The AcroFlex lumbar disc itself (11 mm height × 20 mm diameter) consists of three primary components: two ASTM F-136 implant-grade titanium endplates (Ti-6Al-4V ELI alloy) with sintered titanium beaded ingrowth surfaces, bound together by a hexene-based polyolefin rubber core (Fig. 1). The process of manufacturing of the custom AcroFlex disc was challenging, due to the diminution in size as compared to one that would be implanted in the human intervertebral disc.

Multi-directional flexibility testing

For flexibility assessment, the frozen lumbar specimens were thawed at room temperature, and the surrounding soft tissue and musculature carefully removed to obtain the operative ligamentous functional spinal units (AcroFlex n=20, autograft n=20). Ten intact lumbar motion segments from baboon cadaver spines were evaluated and served as non-operative controls (n=10). For fixation, the superior half of the proximal vertebral body and inferior half of the distal body were secured into rectangular tubing foundations using four, four-point compression screws. Two Plexiglas motion detection markers, each containing three non-co-linear light-emitting diodes designed for detection by an optoelectronic motion measurement system (3020 Optotrak System, Northern Digital Inc, Waterloo, Ontario) were placed on the anterior aspects of the superior and inferior vertebral elements. Using an MTS 858 testing device (MTS Systems, Minneapolis, Minn.) configured with a six-degrees-of-freedom spine simulator, six non-destructive pure moments of flexion/extension ($\pm x$ axis, 4 Nm), lateral bending ($\pm z$ axis, 4 Nm) and axial rotation ($\pm y$ axis, 4 Nm) were applied to the superior end of the vertically oriented specimen, while the caudal portion remained fixed to a testing platform. A total of three load/unload cycles were performed for each motion, with data analysis based on the final cycle. For the six main motions – corresponding to the moments applied – the operative level vertebral rotations (degrees) were quantified in terms of peak range of motion (ROM). To prevent desiccation during assessment, specimens were moistened with 0.9% NaCl sterile irrigation solution.

Histopathologic and histomorphometric analyses

Undecalcified tissue analysis

Following biomechanical analysis, the operative motion segments were processed using undecalcified histologic technique. The motion segments were sectioned in the mid-sagittal plane along the geometric centerline of the intervertebral disc spacer using a Beuhler Isomet saw (Beuhler Inc., Lake Bluff, Ill.). Histologic preparation of the sections included dehydration in 100% ethanol, staining using the Villanueva Osteochrome Bone Stain, undecalcified solution processing and embedding in polymethyl-methacrylate (PMMA). Using the EXAKT Microgrinding Device (EXAKT Technologies, Oklahoma City, Okla.), the embedded specimens were cut to 250- to 300-µm-thick sections, and then ground and polished to 120 µm. Microradiographs were obtained using a Faxitron X-ray Unit and Konica Graphic Arts Film. The slide-

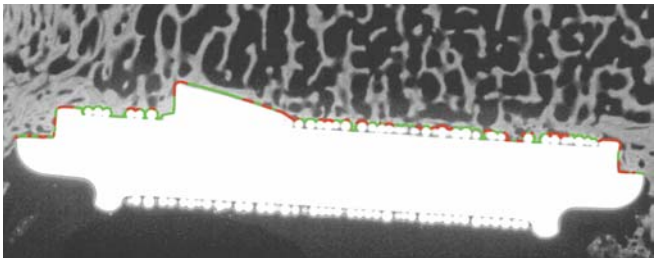

Fig. 3 Microradiograph of the AcroFlex disc prosthesis 6 months post-operatively, demonstrating the histomorphometric method of trabecular ingrowth calculation (% trabecular area/total endplate area)

mounted specimens were placed 12 in. (approx. 30.5 cm) from the beam and exposed for 2 min., using a technique of 45 kV and 3 mA while in direct contact with the single emulsion high-resolution graphics arts film. The resulting high-resolution microradiographs were used for histomorphometric quantification of trabecular bone area at the implant interface. Histopathologic assessment of the slide-mounted undecalcified sections and systemic reticuloendothelial tissues included assessment of particulate wear debris, as well as any signs of inflammatory giant cell reactions, degenerative changes or autolysis.

Using a BioQuant Image Analysis System (R&M Biometrics, Nashville, Tenn.), the high-resolution microradiographs permitted quantification of percentage trabecular ingrowth at the prosthesis-bone interface. The prosthesis surface was manually traced and expressed as a total endplate area pixel count. The regions of trabecular contact were subsequently traced, quantified in pixels and expressed as a percentage of the total endplate area (% ingrowth = apparent bone contact area/gross total endplate area) (Fig. 3).

Data and statistical analysis

For the non-destructive biomechanical analysis, peak ROM for each loading mode was calculated as the sum of motions [displacement (mm) for axial compression or maximum rotation (degrees) for torsion, flexion-extension and lateral bending] occurring in the neutral and elastic zones at the fourth loading cycle. Histomorphometric data represent the percentage of trabecular bone in contact with the AcroFlex (titanium endplates). All data are shown as mean plus/minus one standard deviation and were statistically compared using an analysis of variance (ANOVA) with the Student-Newman-Keuls comparison between groups. Significance was indicated at $P<0.05$.

Results

Surgical procedures

All 20 animals survived the surgery and post-operative time period without incidence of neurologic or infectious complications. The average operative time required was 156±40 min. Average blood loss was 235±35 cc. Assessments of general appearance, ambulation and wound healing were performed for each animal. All animals were characterized as having a normal recovery throughout the post-operative periods. Based on plain film radiographic evaluation and gross histology, all 20 AcroFlex prostheses were solidly fixed – there was no evidence of radiolucency or loosing at a single implant-bone interface (Fig. 4).

Fig. 4 Lateral plain film radiograph obtained 6 months post-operatively, demonstrating position of the AcroFlex device at L5-L6 and autogenous fusion control at L3-L4. Six and 12 months post-operatively, none of the prostheses were subluxed anteriorly or exhibited radiolucencies at the implant-bone interface

Radiographically, seven of the ten autograft levels showed evidence of fusion at 6 months and eight of the ten at 12 months, thus yielding an 80% fusion rate for the autograft group. One animal from the 12-month group was noted to have extravasation of the polyolefin core at the AcroFlex disc level, which was localized in the immediate soft tissue structures. No histopathologic effects were noted in the distant reticuloendothelial/systemic tissues. Implant failure was considered secondary to insufficient curing of the polyolefin core.

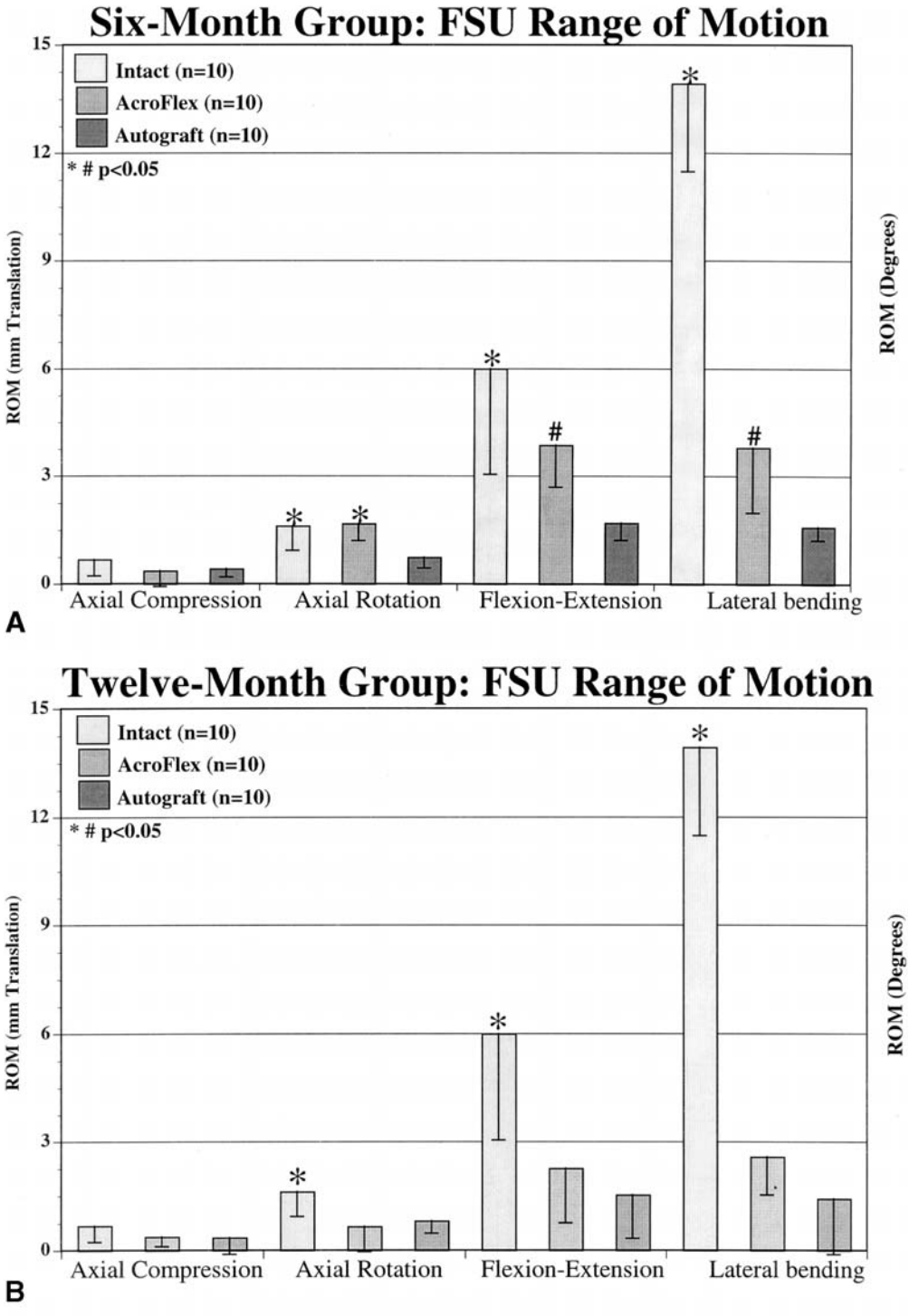

Fig. 5 Multidirectional flexibility testing of the operative functional spinal units was performed 6 (**A**) and 12 (**B**) months post-operatively. At 6 months (**A**), the intact spine and AcroFlex treatments were significantly different from autogenous controls in all loading modes except axial compression ($P<0.05$). Moreover, the intact condition was different from the AcroFlex in flexion/extension and lateral bending ($P<0.05$). At 12 months (**B**), the intact spine was different from the AcroFlex and autograft treatments in all rotational modes ($P<0.05$). Significance is indicated at $P<0.05$ and error bars represent standard deviation

Multi-directional flexibility testing

Six-month treatment groups

Peak ROM comparisons of the 6-month post-operative anterior lumbar interbody fusions, reconstructions with AcroFlex lumbar disc, and non-operative intact motion segments indicated no significant differences in axial compression ($P>0.05$). Axial rotation testing results showed significantly lower ROM for the autograft specimens compared to the AcroFlex and intact treatments ($P<0.05$). The most significant differences in peak ROM were noted between all three treatment groups under flexion/extension and lateral bending loading modalities.

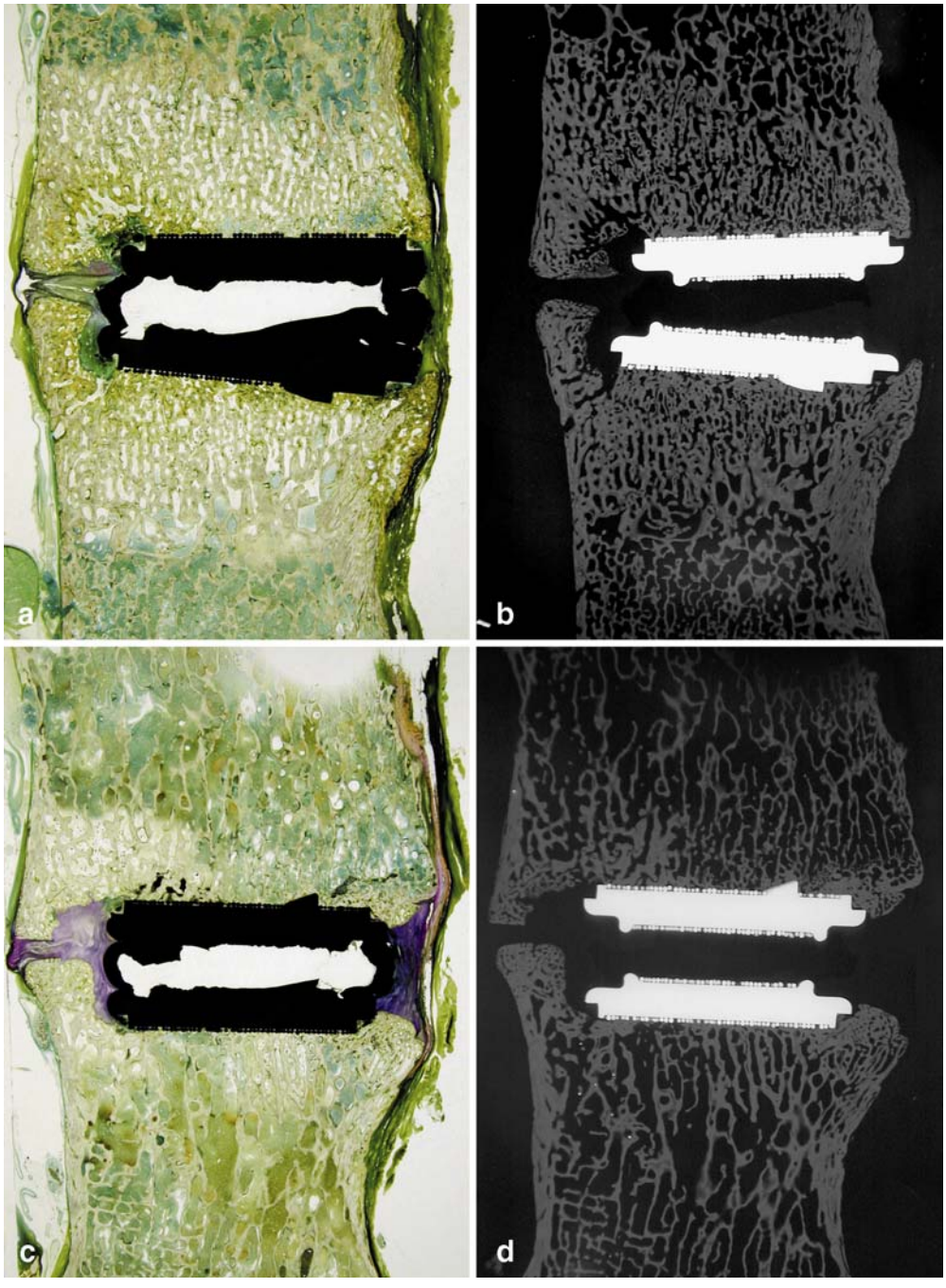

Fig. 6 Undecalcified histologic sagittal sections and corresponding microradiographs obtained from 6-month (**A,B**) and 12-month (**C,D**) treatments. The extent of osseointegration at the bone-metal interface is well demonstrated in these treatments. The absence of the black core is secondary to the cutting and grinding histologic processes necessary for histologic slide production (anterior is to the *right* and posterior *left*; Osteochrome Villanueva Bone Stain)

Specifically, the intact motion segment afforded greater ROM than the AcroFlex treatment, which was significantly different from the autograft fusions (Fig. 5A) (one way ANOVA results: axial compression F=1.10, P= 0.350; axial rotation F=7.64, P=0.003; flexion/extension F=10.36, P=0.000; lateral bending F=105.21, P=0.000).

Twelve-month treatment groups

By the 12-month time interval, the differences in range of motion between the intact spine and AcroFlex treatments had significantly increased. In axial compression, no differences were observed (P>0.05). However, in rotation, flexion-extension and lateral bending the intact spine ROM was significantly greater than the autograft and AcroFlex treatments (P<0.05), which were not statistically different from each other (Fig. 5B) (one way

ANOVA results: axial compression F=1.42, *P*=0.262; axial rotation F=7.36, *P*=0.004; flexion/extension F=15.74, *P*=0.000; lateral bending F=115.36, *P*=0.000).

Undecalcified bone histomorphology

Histopathologic interpretation of the slide-mounted undecalcified specimens indicated no evidence of significant pathologic changes in tissues within or surrounding the AcroFlex lumbar disc prosthesis. Based on plain- and polarized-light microscopic review of the slide-mounted vertebral specimens, there was no evidence of a fibrous or collagenous tissue interface at the prosthesis-bone interface. The trabecular bone in direct contact with the implant was lamellar in structure, without any evidence of sclerosis. Interstitial marrow cavities, devoid of fibrosis, account for the remainder of the implant-bone interface. Histopathologic interpretation of the microradiographs indicated confluent inter-digitization of trabeculae at the prosthetic endplate-bone interface, without evidence of radiolucent lines or gaps (Fig. 6).

The incidence of heterotopic ossification (peri-annular calcification) is observed in many specimens at the 12-month time period and most likely accounts for the decreased ROM observed in multi-directional flexibility testing. The one AcroFlex case demonstrating extravasation of the polyolefin core indicated black wear particles and a localized histiocytic foreign body reaction, without evidence of polymorphonuclear cells. In all remaining cases, there was no incidence of prosthetic endplate migration or evidence of particulate wear debris. Moreover, all histologic specimens were characterized as undergoing a normal healing process, with normal marrow cellularity, osteocyte distribution, osteoid seam widths and without evidence of bone necrosis, inflammatory/giant cell reaction or other significant histopathologic changes.

Histomorphometry

Light microscopic analysis of the 6- and 12-month AcroFlex specimens demonstrated excellent osseointegration at the level of the bone-implant interface (Fig. 3). BioQuant histomorphometric analysis at the metal-bone interface (bone contact area/total endplate area) indicated the mean ingrowth was 54.59±13.24% at 6 months and 56.79±5.85% at 12 months.

Histopathology: systemic/reticuloendothelial tissues

Histologic analysis of the local and systemic tissues at the 6-month interval indicated no significant pathologic changes induced by either AcroFlex disc prosthesis or surgical manipulations. Although no pathology was recorded that could be associated with the AcroFlex lumbar disc device, pre-existing conditions in the animals most likely account for the mild pathologic changes in some tissue structures. For example, the axillary, inguinal, periaortic and mesenteric lymph nodes were characterized as showing mild reactive changes with sinus histiocytosis. In two cases, the presence of eosinophils was noted in axillary nodes. Lungs of all animals with the exception of one showed histiocytic granulomas with tiny polarized particles. These lymph node and lung findings were considered secondary to the environmental housing conditions and unrelated to the implant procedures or materials. The spinal cord sections, based on H&E and Kluver-Barrera (Luxol Blue with PAS) staining methods did not reveal any variations from normal histologic appearance of myelin and nerve cells.

Discussion

The logical progression in the management of joint pathology has been from an immobilizing arthrodesis towards replacement arthroplasty. In the spinal column too, the concept of total disc replacement arthroplasty in order to restore structure and function to the operative motion segment is gaining popular support. A variety of disc designs have been described over the past 35 years, based on the principle of replacing either the nucleus pulposus or the entire disc utilizing a wide assortment of materials in an attempt to replicate the properties of a healthy functional spinal unit [1, 5, 19, 27, 34]. Only a few of these designs have been used in human clinical trials, with varied success [10, 13, 29, 34].

In the current study, radiographic analysis showed no lucencies or loosening of the prosthetic vertebral endplates. A significant decrease in the operative level ROM was observed for the AcroFlex group at 12 months versus the 6-month time period. This was considered secondary to the peri-annular calcification noted in six of ten levels containing the AcroFlex implant at the longer time interval. This anterior ossification is attributed to the custom-made implant having a significantly smaller endplate footprint as compared to the vertebral endplate dimensions (<50%) and limited intrinsic flexibility of the device in the acute post-operative timeframe. Moreover, based on previous studies with the Link Charité III in the same animal model, there was no incidence of peri-annular calcification noted, with operative level ROM equivalent to or greater than intact non-operative controls [20]. Despite the decreased flexibility at the operative levels, there were no issues of debonding of the rubber-titanium interface appreciated radiographically or upon gross inspection. However, extravasation of the polyolefin core did occur in one of the 12-month cases.

Based on the histomorphometry data, definitive trabecular osseointegration of the prosthetic vertebral endplates

appears complete by the 6-month timeframe (54.59%), with only slight increases by the 12-month interval (56.79%). It is important to note that previous studies using hydroxyapatite- (HA)-coated porous ingrowth surfaces (SB Charité III) [20] did not demonstrate an inordinately higher percentage ingrowth (47.9±8.12%) at corresponding time periods versus the sintered titanium beaded surface used in the AcroFlex prosthesis. To put these osseointegration values in perspective, it is useful to look at animal models of porous ingrowth in total hip and total knee arthroplasty. Harvey et al. [14] found the mean ingrowth for femoral stems in a canine model was 9.7± 5.38% for a composite stem and 28.1±5.31% for a titanium alloy stem. Jasty et al. [8, 15] retrieved five femoral stems from patients, and the ingrowth ranged from 4 to 44% (mean 24%). Sumner et al. [31, 33] reported mean ingrowth of bone at 2 years in a canine cementless total hip arthroplasty model. The amount of ingrowth of bone averaged 32.7±4.7% (range 19.7–47.5%) with fiber metal coatings and 24.1±1.8% (range 19.0–31.2%) using bead coatings. Pidhorz et al. [26] retrieved cementless acetabular components in humans, 5 weeks to 75 months post-operatively (mean 41 months) (n=11), and found a mean ingrowth of 12.1±8.2%.

With regard to the quantification methods for osseointegration, there is controversy regarding the most accurate method of measurement of porous ingrowth of cementless prostheses [2, 3, 4, 6]. The three most widely used methods are microradiography, stained histology, and backscattered electron imaging scanning electron microscopy (BEI-SEM) [3]. Turner and co-workers' [32] canine study of femoral component ingrowth most directly approximates our study, as both used microradiography, 6 months post-operative follow-up, and the BioQuant image analysis system. Turner et al.'s microradiographs were made from 100-µm-thick sections, whereas our study utilized 120-µm-thick histology sections. At 6 months, the fiber metal Ti-coated femoral stem in their study showed a 37.3±3% ingrowth of bone, while the figure for the Ti beaded surface femoral stems was 23.3±3.3%.

One potential reason for variability in the quantification of bony ingrowth in total hip replacements is the mismatch between the geometry of the total hip stems and the shape of the surrounding bony cortex – the likelihood of bone ingrowth increases with the proximity of the porous coating to the cortical bone.[9] Other confounding variables include the fact that the porous coating extends different lengths and across different portions of the bone-metal surface in joint components in the extremities [2, 6, 9, 14]. In the SB III Charité and AcroFlex disc replacements studied in our laboratory [7, 20], the porous coating extended across the entire bone-metal interface. Furthermore, in the spine, with total disc replacements there was consistent bony architecture throughout the width and depth of the vertebral body, and the surface was completely flat.

As with joint replacement in the appendicular skeleton, there are a number of clear-cut anatomical and biomechanical considerations in total disc replacement arthroplasty. Foremost, the human functional spine represents a three-joint complex, with segmental rotations and translations occurring along three axes – x, y, z [25]. Moreover, the centers of intervertebral rotation change under flexion/extension and lateral bending conditions, and produce an elliptical instantaneous axis of rotation (IAR) localized in the posterior half and along the inferior endplate of the intervertebral disc [11, 12, 28]. To this end, the device should allow normal, unconstrained physiologic motions; permitting the spine to regulate the device, as opposed to spinal motion adapting to the implant. Additionally, the device must adequately address the in vivo loading conditions [17, 18, 21, 22, 23, 24, 30], must function as a stand-alone implant in the presence of an intact posterior column, and must resist wear, cold flow and material delamination. Most importantly and most challenging is for the device to encourage osseointegration at the bone-metal interface while preserving the biomechanical properties of motion.

The baboon model illustrates a "worst case" scenario, as the animals are not braced or immobilized post-operatively, are rapid to ambulate and perform their natural gymnastics, trapeze utilization and cage rocking within the 1st post-operative week. Moreover, the disc space dimensions (9 mm height, 25 mm depth and 30 mm width) are more accommodating to the smaller human-sized prosthetic implants, with minimal endplate resection required compared to other animal models – sheep, goats or canines [16, 17]. These models can also be used for defining the anatomical feasibility of the surgical approach and instrument design strategies.

This concept of total disc replacement arthroplasty represents a new paradigm in the surgical management of discogenic pathology. As we move from an era of interbody spinal arthrodesis to one in which segmental motion is preserved, this promising new technology offers increasing challenges in the research areas of implant design, spinal kinematics and histologic osseointegration. In the current study, we postulate that the reason for the improved degree of porous osseointegration in total disc replacement prosthesis is due to ligamentotaxis causing sustained compression across the metal-bone interface. Moreover, there were no specific pathologic changes in the local, systemic or reticuloendothelial system to suggest any toxicity or bio-incompatibility issues with regard to implant materials. However, the observed mechanical failure pattern should be considered in future design strategies for total disc replacements. The decreased flexibility properties observed at the 12-month time period appear secondary to implant size, design and implantation technique. This project serves as the first comprehensive in-vivo investigation of the AcroFlex disc prosthesis and establishes an excellent research model in the evaluation of total disc replacement arthroplasty.

References

1. Bao QB, McCullen GM, Higham PA, Dumbleton JH, Yuan HA (1996) The artificial disc: theory, design and materials biomaterials. 17:1157–1167
2. Bloebaum RD, Bachus KN, Jensen JW, Scott DF, Hofman AA (1998) Porous-coated metal backed patellar components in total knee replacement. A postmortem retrieval analysis. J Bone Joint Surg Am 80:518–528
3. Bloebaum RD, Rhodes DM, Rubman MH, Hofman AA (1991) Bilateral tibial components of cementless designs and materials. Microradiographic, backscattered imaging, and histologic analysis. Clin Orthop 268:179–187
4. Buechel FF Sr, Buechel FF Jr, Pappas MJ, D'Alessio J (2001) Twenty-year evaluation of meniscal bearing and rotating platform knee replacements. Clin Orthop 388:41–50
5. Cinotti G, David T, Postacchini F (1996) Results of disc prosthesis after a minimum follow-up period of 2 years. Spine 21:995–1000
6. Collier JP, Mayor MB, Chac JC, Surprenant VA, Surprenant HP, Dauphinais LA (1988) Macroscopic and microscopic evidence of prosthetic fixation with porous-coated materials. Clin Orthop 235:173–180
7. Cunningham BW, Lowery GL, Gonzales V, Orbegoso CM (2001) An analysis of the AcroFlex lumbar disk prosthesis. A non-human primate model. Proceedings of the North American Spine Society. Seattle, Washington, 3 November, pp 74,75
8. Engh CA, Zettl-Schaffer KF, Kukita Y, Sweet D, Jasty M, Bragdon C (1993) Histological and radiographic assessment of well functioning porous-coated acetabular components. A human postmortem study. J Bone Joint Surg Am 75:814–824
9. Engh CA, Hooten JP, Zettl-Shaffer KF, Ghaffarpour M, McGovern TF, Bobyn JD (1995) Evaluation of bone ingrowth in proximally and extensively porous-coated anatomic medullary locking prostheses retrieved at autopsy. J Bone Joint Surg Am 77:903–910
10. Enker P, Steffee A, Mcmillin C, Keppler L, Biscup R, Miller S (1993) Artificial disc replacement. Preliminary report with a 3-year minimum follow-up. Spine 18:1061–1070
11. Gertzbein SD, Chan KH, Tile M, Seligman J, Kapasouri A (1985) Moire patterns: an accurate technique for determination of the locus of the centres of rotation. J Biomech 18:501–509
12. Gertzbein SD, Seligman J, Holtby R, Chan KH, Kapasouri A, Tile M, Cruickshank B (1985) Centrode patterns and segmental instability in degenerative disc disease. Spine 10:257–261
13. Griffith SL, Shelokov AP, Buttner-Janz K, LeMaire JP, Zeegers WS (1994) A multicenter retrospective study of the clinical results of the LINK SB Charite intervertebral prosthesis. The initial European experience. Spine 19:1842–1849
14. Harvey EJ, Bobyn JD, Tanzer M, Stackpool GJ, Krygier JJ, Hacking SA (1999) Effect of flexibility of the femoral stem on bone-remodeling and fixation of the stem in a canine total hip arthroplasty model without cement. J Bone Joint Surg 81:93–107
15. Jasty M, Bragdon CR, Maloney WJ, Haire T, Harris WH (1991) Ingrowth of bone in failed fixation of porous-coated femoral components. J Bone Joint Surg Am 73:1331–1337
16. Kostuik JP (1997) Intervertebral disc replacement. Experimental study. Clin Orthop 337:27–41
17. Kotani Y, Abumi K, Shikinami Y, Takada T, Kadoya K, Shimamoto N, Ito M, Kadosawa T, Fujinaga T, Kaneda K (2002) Artificial intervertebral disc replacement using bioactive three-dimensional fabric: design, development, and preliminary animal study. Spine 27:929–935; discussion 935,936
18. Langrana NA, Parsons JR, Lee CK, Vuono-Hawkins M, Yang SW, Alexander H (1994) Materials and design concepts for an intervertebral disc spacer. I. Fiber-reinforced composite design. J Appl Biomater 5:125–132
19. Lee CK, Langrana NA, Parsons JR, Zimmerman MC (1991) Development of a prosthetic intervertebral disc. Spine 16:S253–S255
20. McAfee PC, Cunningham BW, Orbegoso CM, Sefter JC, Dmitriev AE, Fedder IL. Analysis of porous ingrowth in intervertebral disc prostheses: a non-human primate model. Spine (in press)
21. Nachemson A (1959) Measurement of intradiscal pressure. Acta Orthop Scand Suppl 28:269–289
22. Nachemson A (1960) Lumbar intradiscal pressure. Acta Orthop Scand Suppl 43:1–104
23. Nachemson A (1965) The effect of forward leaning on lumbar intradiscal pressure. Acta Orthop Scand 35:314–328
24. Nachemson A (1966) The load on lumbar disks in different positions of the body. Clin Orthop 45:107–122
25. Panjabi MM (1988) Biomechanical evaluation of spinal fixation devices. I. A conceptual framework. Spine 13:1129–1133
26. Pidhorz LE, Urban RM, Jacobs JJ, Sumner DR, Galante JO (1993) A quantitative study of bone and soft tissues in cementless porous-coated acetabular components retrieved at autopsy. J Arthroplasty 8:213–225
27. Ray CD, Schonmayr R, Kliniken HS (1997) A prosthetic lumbar nucleus "artificial disc". NASS Proceedings 12th Annual Meeting, October 22–25, New York
28. Rolander SD (1966) Motion of the lumbar spine with special reference to the stabilizing effect of posterior fusion. An experimental study on autopsy specimens. Acta Orthop Scand Suppl 90:1–144
29. Ross ESR (1997) A prospective cohort study of the Charite disc replacement. NASS, Proceedings, 12th Annual Meeting, October 22–25, New York
30. Schultz A, Andersson G, Ortengren R, Haderspeck K, Nachemson A (1982) Loads on the lumbar spine. Validation of a biomechanical analysis by measurements. J Bone Joint Surg Am 64: 713–720
31. Sumner DR, Bryan JM, Urban RM, Kuzak JR (1990) Measuring the volume fraction of bone ingrowth: a comparison of three techniques. J Orthop Res 8:448–452
32. Turner TM, Sumner DR, Urban RM, Rivero DP, Galante JO (1986) A comparative study of porous coatings in weight-bearing total hip-arthroplasty model. J Bone Joint Surg Am 68: 1396–1409
33. Urban RM, Jacobs JJ, Sumner DR, Peters CL, Voss FR, Galante JO (1996) The bone- implant interface of femoral stems with non-circumferential porous coating. A study of specimens retrieved at autopsy. J Bone Joint Surg Am 78:1068–1081
34. Zeegers WS, Bohnen LM, Laaper M, Verhaegen MJ (1999) Artificial disc replacement with the modular type SB Charite III: 2-year results in 50 prospectively studied patients Eur Spine J 8:210–217